Continuum interaction in low-energy radiationless transitions

Kh Rezaul Karim and Bernd Crasemann
Department of Physics and Chemical Physics Institute, University of Oregon, Eugene, Oregon 97403
(Received 1 October 1984)

L-shell Coster-Kronig transition rates are calculated for Ar through a formulation which includes the effects of final-state channel mixing. The interchannel interaction changes individual transition rates by as much as 84%. The relative term intensities from the present calculation agree better with experiment than calculations which do not include channel mixing. The discrepancies previously found between measured and calculated total L_1-$L_{2,3}M_1$ Coster-Kronig transition rates and the ratios of L_1-$L_{2,3}M_1$ to L_1-$L_{2,3}M_{2,3}$ and L_1-$L_{2,3}M_1(^1P_1)$ to L_1-$L_{2,3}M_1(^3P_1)$ intensities are largely removed when effects of channel coupling are taken into consideration.

I. INTRODUCTION

Inner-shell vacancy states of atoms decay by radiative and (predominantly) nonradiative processes. The coupling between radiative and radiationless channels has usually been neglected.[1] The electrostatic coupling among the final K-LL Auger channels in Ne was considered by Howat *et al.*,[2,3] and for K-LL, K-LM, and K-MM transitions in Mg by Howat.[4] These authors found that interchannel coupling substantially alters the spectral distribution of the K Auger electrons which are emitted with kinetic energy of several hundred electron volts. It is interesting, therefore, to investigate similar effects in the case of Coster-Kronig processes which are extremely intense, compared with Auger processes, and in which the outgoing electron's kinetic energy is at least an order of magnitude less than in Auger transitions.

One inviting case for theoretical investigation is that of L-shell Coster-Kronig transitions in Ar, for which perplexing discrepancies have existed between experimental results[5,6] and theoretical predictions.[7–11] Hartree,[7] Hartree-Fock-Slater,[8] and Hartree-Fock[9,10] single-configuration calculations have been found to overestimate experimental Ar L_1-$L_{2,3}M_1$ Coster-Kronig rates by factors of ~ 4, the L_1-$L_{2,3}M_1$ to L_1-$L_{2,3}M_{2,3}$ intensity ratio by a factor of ~ 2, and the ratio of L_1-$L_{2,3}M_1(^1P_1)$ to L_1-$L_{2,3}M_1(^3P_1)$ transition rates by a factor of ~ 120. Possible reasons for these striking discrepancies in theoretical predictions include (i) many-body interactions in the initial and final atomic systems, (ii) effects of relaxation in the final ionic state, and (iii) effects of the exchange interaction between the continuum electron and the final bound-state electrons. These possibilities have been investigated in recent calculations.[9–11] A multiconfiguration Dirac-Fock calculation with a limited basis set by Bruneau[11] agrees well with the experimental L_1-$L_{2,3}M_{2,3}$ transition rate, but overestimates the L_1-$L_{2,3}M_1$ rate and the ratios of L_1-$L_{2,3}M_1$ to L_1-$L_{2,3}M_{2,3}$ and L_1-$L_{2,3}M_1(^1P_1)$ to L_1-$L_{2,3}M_1(^3P_1)$ intensities by factors of ~ 4, ~ 3, and ~ 2, respectively. A configuration-interaction Hartree-Fock calculation with a large basis set by Dyall and Larkins,[9] a multiconfiguration Dirac-Fock calculation with an extended basis set by Bruneau,[11] and a multiconfiguration Hartree-Fock calculation including the effects of exchange and relaxation by Karim *et al.*[10] have reduced the discrepancy in the L_1-$L_{2,3}M_1$ rate to about a factor of 2. The discrepancy in the ratio of L_1-$L_{2,3}M_1(^1P_1)$ to the L_1-$L_{2,3}M_1(^3P_1)$ rate is largely removed when spin-orbit interaction in the final ionic state is considered.[11,12] Mehlhorn[13] has recently reevaluated his experimental data, leading to an $\sim 13\%$ decrease in the L_1-$L_{2,3}M_1$ to L_1-$L_{2,3}M_{2,3}$ intensity ratio. This revised experimental ratio agrees better with theoretical predictions, but the discrepancies remain large in comparison with other atomic transition-rate calculations in which theory tends to reach within 10% to 20% of the measured rates. In the work reported here, we have investigated the effects of continuum interaction in the outgoing channels on the total and relative term intensities of Ar L-shell Coster-Kronig transitions.

II. THEORY

Theoretical formulations of radiationless transition rates which include the effects of final-state interchannel interaction have been worked out by Howat *et al.*[3] and by Åberg and Howat.[14] The partial radiationless transition probability from an isolated discrete state ϕ, degenerate with N continuum states $\psi_{\alpha,\epsilon}$, is given to the lowest order in the interaction matrix $V(\epsilon,\epsilon,E)$ by[3,14]

$$W_\alpha = 2\pi \left| \langle \psi_{\alpha\epsilon} | H-E | \phi \rangle + \mathrm{P} \sum_{\beta=1}^{N} \int_0^\infty \frac{\langle \psi_{\beta\tau} | H-E | \phi \rangle V_{\beta\alpha}(\tau,\epsilon,E)}{E-E_\beta-\tau} d\tau - i\pi \sum_{\beta=1}^{N} V_{\beta\alpha}(\epsilon,\epsilon,E) \langle \psi_{\beta\epsilon} | H-E | \phi \rangle \right|^2 , \quad (1)$$

where we have

$$V_{\beta\alpha}(\tau,\epsilon,E)=\langle\psi_{\beta\tau}\,|\,H-E\,|\,\psi_{\alpha\epsilon}\rangle \tag{2}$$

and P denotes the principal value of the integral. The first term in Eq. (1) represents the transition rate in the absence of channel coupling, which reduces to Wentzel's formula[15] if orthogonality of one-electron orbitals between the initial and final states is assumed. The quantities $V_{\beta\alpha}$ are the continuum interaction terms.

The Ar L-shell Coster-Kronig spectrum in LS coupling includes transition from the initial state

$$1s^2 2s\,2p^6 3s^2 3p^6 \tag{3a}$$

to the final states

$$(1)\ 1s^2 2s^2 2p^5 3s(^1P)3p^6 \epsilon p\ ^2S\ , \tag{3b}$$

$$(2)\ 1s^2 2s^2 2p^5 3s(^3P)3p^6 \epsilon p\ ^2S\ , \tag{3c}$$

$$(3)\ 1s^2 2s^2 2p^5 3s^2 3p^5(^3D)\epsilon d\ ^2S\ , \tag{3d}$$

$$(4)\ 1s^2 2s^2 2p^5 3s^2 3p^5(^1D)\epsilon d\ ^2S\ , \tag{3e}$$

$$(5)\ 1s^2 2s^2 2p^5 3s^2 3p^5(^3S)\epsilon s\ ^2S\ , \tag{3f}$$

$$(6)\ 1s^2 2s^2 2p^5 3s^2 3p^5(^1S)\epsilon s\ ^2S\ . \tag{3g}$$

The initial state [Eq. (3a)] can also decay by L_1-MM Auger processes. These channels are extremely weak compared to the preceding Coster-Kronig channels, and are not included in this calculation. The transition matrix elements $\langle\phi\,|\,V\,|\,\psi_{\alpha\epsilon}\rangle$ and the intercontinuum matrix elements $\langle\psi_{\beta\tau}\,|\,V\,|\,\psi_{\alpha\epsilon}\rangle$, where $V=\sum_{i>j}(1/r_{ij})$ is the two-electron interaction operator, can be expressed as a weighted sum of Slater integrals:

$$\langle\psi\,|\,V\,|\,\psi'\rangle=\sum_k a_k R^k(n_1l_1,n_2l_2;n_3'l_3',n_4'l_4')\ .$$

Fano[16] has used Racah algebra to determine the angular coefficients a_k for a many-electron system with several open shells. Fano's formulation has been incorporated in a computer code by Hibbert.[17] We have used Hibbert's program to calculate these coefficients.

III. NUMERICAL CALCULATIONS

The initial and final bound-state one-electron orbitals were generated using the Hartree-Fock computer code of Froese-Fischer.[18] With these known bound-state orbitals, the Hartree-Fock equations for the continuum electrons were obtained. The continuum-electron wave functions were determined in the field of the respective double-hole

TABLE I. Transition matrix elements $\langle\phi\,|\,V\,|\,\psi_{\alpha\epsilon}\rangle$ and intercontinuum matrix elements $\langle\psi_{\alpha\epsilon}\,|\,V\,|\,\psi_{\beta\tau}\rangle$, as defined in Eqs. (1) and (2), for Ar L-shell Coster-Kronig transitions, in LS coupling. Channels are identified as in Eq. (3).

Transition to channel	Matrix element
1	$(\frac{3}{2})^{1/2}R^0(3s\,2p;2s\epsilon p)+(6)^{-1/2}R^1(2p\,3s;2s\epsilon p)$
2	$(\frac{9}{2})^{-1/2}R^0(3s\,2p;2s\epsilon p)-(2)^{-1/2}R^1(2p\,3s;2s\epsilon p)$
3	$-R^1(2p\,3p;2s\epsilon d)+R^1(3p\,2p;2s\epsilon d)$
4	$(3)^{-1/2}[R^1(2p\,3p;2s\epsilon d)+R^1(3p\,2p;2s\epsilon d)]$
5	$(2)^{-1/2}[R^1(2p\,3p;2s\epsilon s)-R^1(3p\,2p;2s\epsilon s)]$
6	$-(6)^{-1/2}[R^1(2p\,3p;2s\epsilon s)+R^1(3p\,2p;2s\epsilon s)]$

Interaction between channels		Matrix element
1	2	$(\frac{27}{4})^{1/2}R^0(2p\epsilon p;\epsilon p\,2p)-(12)^{-1/2}R^1(3s\epsilon p;\epsilon p\,3s)$
1	3	$-(6)^{-1/2}R^1(3p\epsilon p;\epsilon d\,3s)$
1	4	$-[(2)^{1/2}/6][2R^1(3p\epsilon p;3s\epsilon d)-R^1(3p\epsilon p;\epsilon d\,3s)]$
1	5	$(12)^{-1/2}R^1(3p\epsilon p;\epsilon s\,3s)$
1	6	$(\frac{1}{6})[2R^1(3p\epsilon p;3s\epsilon s)-R^1(3p\epsilon p;\epsilon s\,3s)]$
2	3	$-(\frac{2}{9})^{1/2}R^1(3p\epsilon p;3s\epsilon d)+(2)^{-1/2}R^1(3p\epsilon p;\epsilon d\,3s)$
2	4	$-(6)^{-1/2}R^1(3p\epsilon p;\epsilon d\,3s)$
2	5	$(\frac{1}{3})R^1(3p\epsilon p;3s\epsilon s)-(1/2)R^1(3p\epsilon p;\epsilon s\,3s)$
2	6	$(12)^{-1/2}R^1(3p\epsilon p;\epsilon s\,3s)$
3	4	$(3)^{-1/2}[R^1(2p\epsilon d;\epsilon d\,2p)-R^1(3p\epsilon d;\epsilon d\,3p)]$
3	5	$(\frac{2}{25})^{1/2}[R^2(2p\epsilon d;2p\epsilon s)+R^2(3p\epsilon d;3p\epsilon s)]$ $-(2)^{-1/2}[R^1(2p\epsilon d;\epsilon s\,2p)+R^1(3p\epsilon d;\epsilon s\,3p)]$
3	6	$(6)^{-1/2}[R^1(3p\epsilon d;\epsilon s\,3p)-R^1(2p\epsilon d;\epsilon s\,2p)]$
4	5	$(6)^{-1/2}[R^1(3p\epsilon d;\epsilon s\,3p)-R^1(2p\epsilon d;\epsilon s\,2p)]$
4	6	$(\frac{2}{25})^{1/2}[R^2(2p\epsilon d;2p\epsilon s)+R^2(3p\epsilon d;3p\epsilon s)]$ $-(18)^{-1/2}[R^1(2p\epsilon d;\epsilon s\,2p)+R^1(3p\epsilon d;\epsilon s\,3p)]$
5	6	$(12)^{-1/2}[R^1(2p\epsilon s;\epsilon s\,2p)-R^1(3p\epsilon s;\epsilon s\,3p)]$

ionic states. Orthogonality between the initial- and final-state one-electron orbitals was assumed. Experimental continuum-electron energies were used for the resonance energies in Eq. (1). The contribution of the imaginary part of Eq. (1) is negligible. An upper limit of 80 a.u. was found appropriate. The principal-value integrations were performed by methods suggested by Bloch[19] and Amusia *et al.*[20]

IV. RESULTS AND DISCUSSION

The transition and intercontinuum matrix elements for Coster-Kronig channels that deexcite the $2s$ vacancy state of Ar are listed in Table I. Final ionic-state coupling is neglected. The transition amplitude $\langle\phi \mid V \mid \psi_{\beta\tau}\rangle$ and the intercontinuum matrix elements $\langle\psi_{\alpha\epsilon} \mid V \mid \psi_{\beta\tau}\rangle$ for the channel $(2p\,3s)^1P\epsilon p\,^2S$, with all other channels [$\beta=1,\alpha=2,3,4,5,6$ as in Eq. (3)], are plotted as functions of continuum-electron energy τ in Fig. 1. The matrix elements vary smoothly and get smaller as τ increases. This, and the fact that continuum-electron energies of Ar L-shell Coster-Kronig electrons are all <2 a.u., make the integrand in Eq. (1) negligible at higher energy. Other transition and intercontinuum matrix elements exhibit similar behavior.

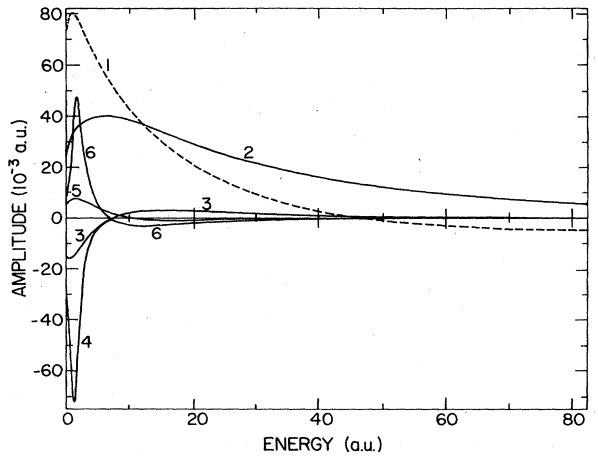

FIG. 1. Calculated transition matrix element $\langle\phi \mid V \mid \psi_{\beta\tau}\rangle$ (dashed line) and intercontinuum matrix elements $\langle\psi_{\alpha\epsilon} \mid V \mid \psi_{\beta\tau}\rangle$ between channel $(2p\,3s)^1P\epsilon p\,^2S$ and other channels [$\beta=1,\alpha=2,3,4,5,6$ as in Eq. (3)] as function of continuum-electron energy.

A. Effects on relative intensities

The contributions to the transition amplitudes due to intercontinuum interaction are listed in Table II. The Hartree-Fock results based on Wentzel's ansatz [first term in Eq. (1)] are also listed for comparison. The individual correction terms from channel mixing vary greatly in magnitude and in phase and are substantially larger than those obtained by Howat *et al.*[2,3] for K-LL Auger transitions in Ne. The transition rates based on this calculation are listed in Table III with corresponding experimental rates. The Hartree-Fock results are included for comparison.

The overall effect of channel mixing is to redistribute the intensity among component channels without significant change in the total intensity. There is a substantial transfer of intensity from the L_1-$L_{2,3}M_1$ channel to L_1-$L_{2,3}M_{2,3}$ channels. This brings the ratio of L_1-$L_{2,3}M_1$ to L_1-$L_{2,3}M_{2,3}$ rates to within $\sim 50\%$ of the experimental value. The Hartree-Fock calculation overestimates this ratio by a factor of 2. The individual transition rates change by as little as $\sim 3\%$ for the L_1-$L_{2,3}M_{2,3}(^3D)$ rate to as much as $\sim 84\%$ for the L_1-$L_{2,3}M_1(^3P)$ rate. The major change in the latter rate is related to the fact that Hartree-Fock theory in LS coupling grossly underestimates the intensity of this particular line. The ratios of individual transition rates to the total L_1-$L_{2,3}M_{2,3}$ rate from the present calculation agree better with measurements than the Hartree-Fock results.

TABLE II. Transition amplitudes and correction terms (in 10^{-3} a.u.) due to interchannel interaction in Ar L-shell Coster-Kronig transitions. Channels are identified as in Eq. (3).

Channels	1	2	3	4	5	6
1		−7.006	0.604	4.556	−0.867	−6.964
2	−2.778		0.346	0.335	0.365	−0.153
3	4.201	2.681		4.226	0.465	−2.557
4	−3.851	−2.390	−0.327		1.889	0.012
5	0.161	2.444	0.371	0.254		−0.217
6	−2.655	−0.032	0.171	−0.615	0.211	
Total	−4.922	−4.303	1.165	8.756	2.063	−9.879
Amplitude without channel mixing	80.059	−12.111	−76.973	43.605	34.758	−39.576
Corrected amplitude	75.137	−16.414	−75.808	52.361	36.821	−49.455

TABLE III. Transition rates (in 10^{-3} a.u.) in the L_1-$L_{2,3}M$ Coster-Kronig spectrum of Ar.

Final vacancies		Transition rate Theory[b]	Theory[c]	Expt.[d]	Expt.[e]	Relative intensity[a] Theory[b]	Theory[c]	Expt.[d]
$L_{2,3}M_1$	^1P	40.27	35.47	7.6		60.5	45.9	14.9
	^3P	0.92	1.69	5.8		1.4	2.2	11.4
	Sum	41.19	37.16	13.4	14.4±4.5	61.8	48.1	26.3
$L_{2,3}M_{2,3}$	^3D	37.23	36.11	24.9		55.9	46.8	48.8
	^1D	11.95	17.23	7.0		17.9	22.3	13.7
	^3P			4.0				7.8
	^1P			0.8				1.6
	^3S	7.59	8.52	4.2		11.4	11.0	8.2
	^1S	9.84	15.36	10.1		14.8	19.9	19.8
	Sum	66.61	77.22	51.0	47.1±10	100.0	100.0	100.0

[a]Normalized to L_1-$L_{2,3}M_{2,3}=1$.
[b]Nonrelativistic single-configuration Hartree-Fock calculations.
[c]Nonrelativistic single-configuration Hartree-Fock calculation corrected for channel coupling.
[d]Reference 5.
[e]Reference 13.

B. Effects on the L_1-$L_{2,3}M_1$ rate

Hartree-Fock calculations in LS coupling overestimate the total L_1-$L_{2,3}M_1$ rate by a factor of 4 and the ratio of the L_1-$L_{2,3}M_1(^1P_1)$ to the L_1-$L_{2,3}M_1(^3P_1)$ rate by a factor of 122. The effects of electron correlation, atomic relaxation, exchange interaction of the continuum electrons with the core, and spin-orbit interaction between $(^1P_1)$ and $(^3P_1)$ ionic states were investigated in our earlier papers.[10,12] We now also include the effects of channel mixing. The total L_1-$L_{2,3}M_1$ transition rate and the ratio of $(^1P_1)$ to $(^3P_1)$ line intensities are reported in Table IV, where the correction terms from channel mixing are included. The total L_1-$L_{2,3}M_1$ rate decreases by $\sim 10\%$ and the ratio of $(^1P_1)$ to $(^3P_1)$ rates decreases by $\sim 3\%$ because of interchannel coupling. It is seen that the discrepancies between experimental values and theoretical predictions are progressively reduced as we include these correction terms. Good agreement in the relative term intensities is found. The total L_1-$L_{2,3}M_1$ rate is now within $\sim 55\%$ of the experimental rate. Taking into ac-

TABLE IV. Transition rates in m a.u. (1m a.u.$=0.027\,21$ eV/$\hbar=4.134\times10^{13}$ s^{-1}) of the L_1-$L_{2,3}M_1$ Coster-Kronig spectrum of Ar.

Source	Transition rate $^1P_1$	$^3P_1$	Total rate	$^1P_1$ to $^3P_1$ ratio
Experiment[a]	7.6	5.8	13.4	1.31
Experiment[b]			14.4±4.5	
Dyall and Larkins[c]	23.75	0.21[d]	23.96	114.92
Bruneau[e]	34.33	13.63	47.96	2.52
Present work (I)[f]	40.27	0.31	40.58	129.90
Present work (II)[g]	35.47	0.86	36.33	41.24
Present work (III)[h]	26.78	13.80	40.58	1.94
Present work (IV)[i]	23.93	12.40	36.33	1.93
Present work (V)[j]	14.66	7.84	22.50	1.87

[a]Reference 5.
[b]Reference 13.
[c]Nonrelativistic Hartree-Fock calculation with configuration interaction (Ref. 9).
[d]This rate is one-third of the rate reported by the authors of Ref. 8 for transition to the ^3P state; it has been shown (Ref. 12) that one-third of the ^3P intensity pertains to the $^3P_1$ channel.
[e]Multiconfiguration Dirac-Fock calculation with a limited basis set (Ref. 11).
[f]Nonrelativistic single-configuration Hartree-Fock calculation.
[g]Nonrelativistic single-configuration Hartree-Fock calculation corrected for channel coupling.
[h]Nonrelativistic single-configuration Hartree-Fock calculation in intermediate coupling.
[i]Nonrelativistic single-configuration Hartree-Fock calculation corrected for spin-orbit and channel-coupling effects.
[j]Nonrelativistic relaxed-orbital multiconfiguration Hartree-Fock calculation including effects of exchange [transition matrix elements in the first term of Eq. (1) taken from Ref. 10], corrected for spin-orbit and channel-coupling effects.

count a 31% uncertainty in the measured results,[13] the present calculation agrees well with experiment.

C. Effects on the L_1-$L_{2,3}M_{2,3}$ and total rates

The present Hartree-Fock calculation leads one to overestimate the total measured L_1-$L_{2,3}M_{2,3}$ rate by $\sim 30\%$. Interchannel interaction increases this rate by $\sim 16\%$ and the total rate by $\sim 6\%$. Since channel coupling shifts some intensity from L_1-$L_{2,3}M_1$ to L_1-$L_{2,3}M_{2,3}$ transitions, the disagreement of the total L_1-$L_{2,3}M_{2,3}$ rate is enhanced. Bruneau[11] has shown, however, that relativity plays an important role in the Ar L_1-$L_{2,3}M_{2,3}$ spectra. The total rate from a multiconfiguration Dirac-Fock calculation with a limited basis set[11] for these channels differs by only $\sim 2\%$ from the experimental value. Dyall and Larkins[9] have found this rate to decrease by $\sim 8\%$, when a large number of configuration-state functions are included in the calculation. A multiconfiguration Dirac-Fock calculation with an extended basis set as of Dyall and Larkins[9] is expected to underestimate the total L_1-$L_{2,3}M_{2,3}$ rate by a few percent; an increase in the intensity of this line because of channel coupling will thus largely be compensated, and the calculated values for the total L_1-$L_{2,3}M_{2,3}$ and L_1-$L_{2,3}M$ rates can be expected to lie within the limits of experimental uncertainty.

V. CONCLUSION

The distribution of low-energy radiationless transition intensities can be significantly altered by continuum interaction among channels. For L-shell Coster-Kronig transitions in Ar, the individual transition rates can be affected by as much as $\sim 84\%$. These changes are substantially larger than those in Auger processes, in which term intensities are affected by 10—40 %. Relative term intensities from the present calculations agree better with experiment than calculations which do not include channel mixing. The overall effect of channel mixing is to redistribute the intensity in component channels without significantly altering the total intensity.

ACKNOWLEDGMENTS

We are indebted to M. H. Chen for his collaboration in the initial stages of this investigation and to T. Åberg for constructive comments on the manuscript. We thank W. Mehlhorn for helpful correspondence. This work was supported in part by the Advanced Research Projects Agency of the U.S. Department of Defense, monitored by the U.S. Air Force Office of Scientific Research under Contract No. F49620-84-C-0039.

[1]For the effects of interference between radiative and radiationless channels, however, see L. Armstrong, Jr., C. E. Theodosiou, and M. J. Wall, Phys. Rev. A **18**, 2538 (1978); V. L. Jacobs, Phys. Rev. A **31**, 383 (1985).

[2]G. Howat, T. Åberg, O. Goscinski, S. C. Soong, C. P. Bhalla, and M. Ahmed, Phys. Lett. **60A**, 404 (1977); G. Howat, T. Åberg, and O. Goscinski, in Abstracts of the Proceedings of the International Conference on X-ray Spectra, Gaithersburg, 1976 (unpublished), p. 35.

[3]G. Howat, T. Åberg, and O. Goscinski, J. Phys. B **11**, 1575 (1978).

[4]G. Howat, J. Phys. B **11**, 1589 (1978).

[5]W. Mehlhorn, Z. Phys. **208**, 1 (1968).

[6]J. Nordgren, H. Ågren, L. Selander, C. Nordling, and K. Siegbahn, Phys. Scr. **16**, 70 (1977); **19**, 5 (1979).

[7]A. Rubenstein, Ph.D. thesis, University of Illinois, Urbana, 1955 (unpublished).

[8]E. J. McGuire, in *Atomic Inner-Shell Processes,* edited by B. Crasemann (Academic, New York, 1975), Vol. I, p. 293; Phys. Rev. A **3**, 1801 (1971).

[9]K. G. Dyall and F. P. Larkins, J. Phys. B **5**, 4103 (1982).

[10]K. R. Karim, M. H. Chen, and B. Crasemann, Phys. Rev. A **29**, 2605 (1984).

[11]J. Bruneau, J. Phys. B **16**, 4135 (1983).

[12]K. R. Karim and B. Crasemann, Phys. Rev. A **30**, 1107 (1984).

[13]W. Mehlhorn (private communication).

[14]T. Åberg and G. Howat, in *Handbuch der Physik,* edited by W. Mehlhorn (Springer, Berlin, 1982), Vol. 31, p. 469.

[15]A. Wentzel, Z. Phys. **43**, 524 (1927).

[16]U. Fano, Phys. Rev. **140**, A67 (1965).

[17]A. Hibbert, Comput. Phys. Commun. **2**, 180 (1971).

[18]C. Froese-Fischer, Comput. Phys. Commun. **14**, 145 (1978).

[19]C. Bloch, *Many-Body Description of Nuclear Structure and Reactions, Proceedings of the International School of Physics "Enrico Fermi," Course XXXVI,* edited by C. Bloch (Academic, London, 1966), p. 394.

[20]M. Ya. Amusia and N. A. Cherepkov, Case Stud. At. Phys. **5**, 47 (1975).